2.C

Nuclear Physics **A124** (1969) 177—198; © *North-Holland Publishing Co., Amsterdam*

ACCURATE CALCULATION OF THE REACTION MATRIX IN LIGHT NUCLEI AND IN NUCLEAR MATTER

A. KALLIO † and B. D. DAY

Argonne National Laboratory, Argonne, Illinois ††

Received 9 September 1968

Abstract: A method for calculating the Brueckner reaction matrix in the oscillator representation, which was outlined in an earlier letter, is explained in detail. The basic equations are derived and solved numerically. It is shown how the t-matrix elements thus obtained can be used to calculate certain higher-order diagrams for the energy and r.m.s. radius; and numerical results are presented. Finally, the method is applied to infinite nuclear matter, and some numerical results are given for the Reid hard-core and soft-core potentials.

1. Introduction

In a previous letter [1]), a method for calculating the nuclear reaction matrix in the oscillator representation was outlined. The present paper gives more detailed information about the method including its derivation, its convergence properties and its use in actual nuclear calculations. It is also shown that the method can be used for infinite nuclear matter, and some illustrative numerical calculations are presented.

The basic idea of the present method is the same as that of Eden and Emery [2]). We improve on the Eden-Emery method by deriving a better treatment of the Pauli operator and by giving a simple and accurate iteration procedure for solving the basic integro-differential equation. Numerical calculations using our improved treatment of the Pauli operator have also been performed by Grillot and McManus [3]) (although they solved the integro-differential equation in a different way), and the original Eden-Emery method has been investigated by Becker and collaborators [4]).

2. Basic equation

We shall first consider the Brueckner-Hartree-Fock calculation of light nuclei employing central forces only. For simplicity, the tensor force is studied only in the nuclear-matter case. In the case of light nuclei, certain results of the Brueckner-Hartree-Fock calculation can be compared with the result of a variational calculation [5]) employing the very same central interaction with hard core.

In the present treatment, we want to escape the Hartree-Fock part of the calculation as easily as possible. To this end, we use some of the qualitative results of a recent

† Present address: Department of Theoretical Physics, University of Oulu, Oulu, Finland.

†† Work performed under the auspices of the U.S. Atomic Energy Commission.

calculation [6]), which employed a parameterized effective interaction fixed so as to give the properties of nuclear matter correctly. We believe that our effective interaction is sufficiently close to it that the qualitative features are the same. In that calculation, the single-particle wave functions were expanded in the oscillator basis, the expansion coefficients being treated as variational parameters which were determined from the Hartree-Fock conditions. The features most useful to us are that (i) the total energy was found to be insensitive to the number of parameters included in the expansion, (ii) the Hartree-Fock potential is non-local, and (iii) the single-particle wave functions $\langle r|nl\rangle$ are quite close to the oscillator functions with the same quantum numbers nl at least for a suitable choice of the oscillator parameter. From this, we conclude that it is unnecessary to perform the Hartree-Fock part of the calculations exactly, since one only gains a couple of MeV for the whole nucleus in doing so. The errors that arise from the inaccuracies in the reaction matrix elements are usually larger. Instead of trying to solve the whole self-consistency problem by varying the wave functions, we parametrize the Hartree-Fock Hamiltonian. Here we can follow the procedure suggested by Eden and Emery [2]) and write the single-particle Hamiltonian in the form

$$H = H_0 + \sum_n C_n|n\rangle\langle n| = T + U_0 + \sum_n c_n|n\rangle\langle n|, \tag{1}$$

where H_0 is some known single-particle Hamiltonian, and the corresponding state vectors $|n\rangle$ are the same for both Hamiltonians H and H_0. It is seen that the Hamiltonian H is non-local as is required, yet the single-particle wave functions are independent of the parameters C_n, which are to be determined from well-defined Hartree-Fock conditions †.

In the Brueckner method, one should have a Hartree-Fock self-consistency condition for occupied states and a different condition for intermediate states. Recent developments [7]) in nuclear-matter calculations have shown that there is no simple condition for intermediate states, because the diagram one previously canceled out with a suitable choice of the single-particle potential is now absorbed into the three-body cluster summation. Since this three-body cluster contribution is very small in nuclear matter, it is likely to be small also in finite nuclei. Then for intermediate states in nuclear matter, one would use the kinetic energy only. When using Hamiltonian (1) for finite nuclei, it is natural to choose $C_m = 0$ for intermediate states. For the occupied states, the parameters C_m are to be calculated from the conditions

$$\langle n|U|n\rangle = \sum_{m \leqq A} \langle mn|t|mn - nm\rangle \tag{2}$$

$$= \langle n|U_0|n\rangle + C_n, \tag{3}$$

$$t = v - v\frac{Q}{e}t. \tag{4}$$

† The single-particle wave functions will later be corrected (sect. 5) by calculating higher-order terms.

The self-consistency conditions for occupied states become almost trivial in the present model. However, the t-matrix elements will depend upon the parameters C_n, and one has to calculate these in a self-consistent way. To see this, let us write down the t-matrix equation (4) corresponding to an unperturbed state $|\phi\rangle = |mn\rangle$, with total energy $E_0 = E_m + E_n$ relative to the Hamiltonian H_0. Defining the correlated state vector $|\psi\rangle$ by

$$t|\phi\rangle = v|\psi\rangle, \tag{5}$$

we obtain from (4) the integral equation

$$|\psi\rangle = |\phi\rangle - \frac{Q}{e} v|\psi\rangle, \tag{6}$$

where

$$e = H_0(1, 2) - E_0 - \Delta. \tag{7}$$

Here H_0 (1, 2) is the two-body model Hamiltonian which satisfies

$$H_0(1, 2)|\phi\rangle = E_0|\phi\rangle, \tag{8}$$

and Δ is given by

$$\Delta = C_m + C_n. \tag{9}$$

Instead of eq. (6) we can also use the Bethe-Goldstone integro-differential equation which is obtained from eq. (6) by multiplying from the left with the operator e of eq. (7) and then "saturating" from the left by $\langle \boldsymbol{rR}|$. The equation becomes

$$[E_0 + \Delta - H_0(1, 2)]\psi(\boldsymbol{r}, \boldsymbol{R}) = \Delta\phi(\boldsymbol{r}, \boldsymbol{R}) + \langle \boldsymbol{rR}|Qv|\psi\rangle, \tag{10}$$

which is an integro-differential equation for the function

$$\langle \boldsymbol{rR}|\psi\rangle = \psi(\boldsymbol{r}, \boldsymbol{R}). \tag{11}$$

Here $\boldsymbol{r}$ and $\boldsymbol{R}$ are the relative and center-of-mass vectors for the two particles. This equation is equivalent to the original t-matrix equation (4); and for the t-matrix elements, we obtain from eq. (5)

$$\langle mn|t|mn\rangle = \langle \phi|v|\psi\rangle = \langle \phi|t|\phi\rangle. \tag{12}$$

It is clear from eq. (10) that ψ depends upon Δ and hence upon the C_n. What one does in practice is to calculate the t-matrix elements (12) for a few values of Δ and interpolate to satisfy eqs. (2) and (3).

Thus far our discussion is true for any local potential $U_0(r)$. In the next sections, we shall study in detail how this model works if we select the oscillator potential. It should be pointed out that eq. (10) reduces to the reference-spectrum equation [8]) if we set $Q = 1$. One of the purposes of the present paper is to study various approximations for the Pauli operator Q.

3. Bethe-Goldstone equation

In order to perform numerical calculations, we now specialize to the oscillator case, which is the only model for which one can perform calculations with sufficient accuracy. Eden and Emery [2]) have derived a useful approximation for treating the Pauli principle. One of the purposes of the present study is to investigate the accuracy of their approximation. Furthermore we shall present a numerical iteration method by which the radial integro-differential equations can be solved exactly.

For the oscillator case, we can use the expansions

$$\phi(\boldsymbol{r}, \boldsymbol{R}) = \sum_{nlNL} \langle n_1 l_1 n_2 l_2, \Lambda | nlNL, \Lambda \rangle [\phi_{nl}(\boldsymbol{r})\phi_{NL}(\boldsymbol{R})]^{\Lambda},$$

$$\psi(\boldsymbol{r}, \boldsymbol{R}) = \sum_{nlNL} \langle n_1 l_1 n_2 l_2, \Lambda | nlNL, \Lambda \rangle [\psi_{nl}^{NL\Lambda}(\boldsymbol{r})\phi_{NL}(\boldsymbol{R})]^{\Lambda}. \tag{13}$$

In order to be able to separate out the c.m. motion, we make two assumptions. (i) In the expansion (13) of $\psi(\boldsymbol{r}, \boldsymbol{R})$, we need to take only the same number of terms as in the expansion of $\phi(\boldsymbol{r}, \boldsymbol{R})$. (ii) The parameter Δ and the relative Bethe-Goldstone wave function $\psi_{nl}^{NL\Lambda}(\boldsymbol{r})$ depend only upon quantum numbers $nlNL$, Λ and not upon $n_1 l_1 n_2 l_2$ individually. The validity of these assumptions will be further discussed in sect. 7.

If we substitute (13) into eq. (10), multiply both sides with the Moshinsky bracket $\langle n_1 l_1 n_2 l_2, \Lambda | n'l'N'L', \Lambda \rangle$ and sum over $n_1 l_1 n_2 l_2$, the orthogonality of the brackets in the component wave functions

$$\phi = [\phi_{nl}(\boldsymbol{r})\phi_{NL}(\boldsymbol{R})]^{\Lambda},$$

$$\psi = [\psi_{nl}^{NL\Lambda}(\boldsymbol{r})\phi_{NL}(\boldsymbol{R})]^{\Lambda} \tag{14}$$

gives

$$[E_0 + \Delta - H_0(r) - H_0(R)]\psi = \Delta\phi + v\psi - \langle \boldsymbol{rR}|(1-Q)v|\psi\rangle. \tag{15}$$

Next we shall derive the radial equation for central forces. Multiply eq. (15) from the left by

$$[Y_l^*(\hat{\boldsymbol{r}})\phi_{NL}^*(\boldsymbol{R})]^{\Lambda} \tag{16}$$

and integrate both sides over $\boldsymbol{R}$ and $\hat{\boldsymbol{r}}$. However, first we have to calculate the Pauli term

$$F(\boldsymbol{r}, \boldsymbol{R}) = \langle \boldsymbol{rR}|(1-Q)v|\psi\rangle$$

$$= \sum_{n_1 l_1 n_2 l_2}{}' \langle \boldsymbol{rR}|n_1 l_1 n_2 l_2, \Lambda\rangle\langle n_1 l_1 n_2 l_2, \Lambda|v|\psi\rangle. \tag{17}$$

Here the prime on the summation sign means that at least one of the states $(n_1 l_1)$, $(n_2 l_2)$ is occupied. Similar ideas have been used by Wong [9]). Next we make the expansions

$$|n_1 l_1 n_2 l_2, \Lambda\rangle = \sum_{\substack{n'l' \\ N'L'}} \langle n_1 l_1 n_2 l_2, \Lambda | n'l'N'L', \Lambda\rangle |n'l'N'L', \Lambda\rangle,$$

$$\langle n_1 l_1 n_2 l_2, \Lambda|v|\psi\rangle = \sum_{n''} \langle n_1 l_1 n_2 l_2, \Lambda | n''lNL, \Lambda\rangle\langle n''l|v|\psi_{nl}^{NL\Lambda}\rangle$$

to obtain

$$F(\boldsymbol{r}, \boldsymbol{R}) = \sum_{n''} \sum_{\substack{n'l' \\ N'L'}} \sum_{\substack{n_1 l_1 \\ n_2 l_2}}' \langle n_1 l_1 n_2 l_2, \Lambda | n'l'N'L', \Lambda \rangle \langle n_1 l_1 n_2 l_2, \Lambda | n''lNL, \Lambda \rangle$$
$$\times \langle n''l|v|\psi_{nl}^{NL\Lambda}\rangle [\phi_{n'l'}(\boldsymbol{r})\phi_{N'L'}(\boldsymbol{R})]^{\Lambda}.$$

When the integration (16) is performed, orthogonality requires that $N' = N$, $L' = L$, and $l' = l$. Furthermore the energy conservation in the Moshinsky transformation implies that $n'' = n'$. If we define

$$P_l^{NL\Lambda}(n') = \sum_{\substack{n_1 l_1 \\ n_2 l_2}}' \langle n_1 l_1 n_2 l_2, \Lambda | n'lNL, \Lambda \rangle^2,$$
$$F(r) = \sum_{n'} P_l^{NL\Lambda}(n') \langle n'l|v|\psi_{nl}^{NL\Lambda}\rangle \phi_{n'l}(r), \tag{18}$$

we finally obtain the radial equation in the form

$$[\varepsilon_{nl} + \Delta - H_0(r)]\psi_{nl}^{NL\Lambda}(r) = \Delta\phi_{nl}(r) + v\psi_{nl}^{NL\Lambda}(r) - F(r). \tag{19a}$$

Here $\phi_{nl}(r)$ and $\psi_{nl}^{NL\Lambda}(r)$ are respectively the unperturbed and perturbed radial functions multiplied by r and the radial Hamiltonian $H_0(r)$ is

$$H_0(r) = -\frac{\hbar^2}{2\mu}\left[\frac{\mathrm{d}^2}{\mathrm{d}r^2} - \frac{l(l+1)}{r^2}\right] + \tfrac{1}{2}\mu\omega^2 r^2,$$

whose eigenvalues are ε_{nl}.

4. Method of solution

In order to discuss the solution of eq. (19), we rewrite it with somewhat simplied notation as

$$[\varepsilon + \Delta - H_0(r)]\psi(r) = \Delta\phi(r) + v\psi(r) - \sum_{n'} P(n')\langle n'|v|\psi\rangle\phi_{n'}(r). \tag{19b}$$

This is an integro-differential equation of second order. For a potential containing a hard core, the wave-function ψ should satisfy the boundary conditions

$$\psi(r) = 0 \qquad \text{for} \quad r < c, \tag{20}$$

$$\lim_{r\to\infty} \psi(r) = 0. \tag{21}$$

Also ψ should be normalized according to

$$\langle\phi|\psi\rangle = 1. \tag{22}$$

This condition is automatically satisfied if ψ is a solution of eq. (19). To see this, we multiply eq. (19) from the left by $\phi(r)$ and integrate over r. As a result of the hermiticity of $H_0(r)$, we obtain

$$\Delta\langle\phi|\psi\rangle = \Delta + \langle\phi|v|\psi\rangle - P(n)\langle\phi|v|\psi\rangle.$$

Now for the initial state $\phi = \phi_n$, we always have $P(n) = 1$. Therefore for non-vanishing Δ, condition (22) is satisfied.

The particular method of solution used in the present paper is based on the following facts. In formula (18) for $F(r)$, one needs to take only a few terms in the summation because, even though $\langle n'|v|\psi\rangle$ is appreciable for quite large n', the $P(n')$ rapidly go to zero with increasing n' (as can be seen in table 1). For light nuclei up to ^{40}Ca, only the values $n' = 0, 1, 2, 3, 4$ need to be included.

TABLE 1

Comparison between the numbers $P_l^{NL\Delta}(n)$ for ^{16}O and the values from the Eden-Emery approximation

n	$P_0^{000}(n)$	$P_0^{100}(n)$	Eden-Emery
0	1	1	1
1	1	0.418	1
2	0.625	0.365	0
3	0.203	0.274	0

The solution can be constructed by iteration using a sequence of non-homogeneous differential equations, $\Delta\phi(r) - F(r)$ being the non-homogeneous term which we assume to be a known function from the previous iteration. At each stage of iteration, the general solution of the full equation is obtained by adding a particular solution to the general solution of the homogeneous equation, which of course remains the same throughout the iteration. In practice, this is performed numerically by starting with asymptotic solutions for large r and integrating inward to the hard-core radius.

The asymptotic form of the solution ψ_h of the homogeneous equation satisfying the boundary condition (21) can be expressed in terms of Weber functions [10]. The inhomogeneous equation has an asymptotic solution of the form

$$\psi_i \underset{r\to\infty}{\to} \sum C_{n'}\phi_{n'}(r),$$

$$C_{n'} = -\frac{P(n')\langle n'|v|\psi_n\rangle}{\varepsilon_{nl} - \varepsilon_{n'l} + \Delta} \qquad \text{for} \quad n' \neq n,$$

$$C_n = 1 - \frac{\langle n|v|\psi_n\rangle}{\Delta}.$$

The general solution is then of the form

$$\psi(r) = A\psi_h(r) + \psi_i(r), \tag{23}$$

where the constant A is determined in such a way that $\psi(r)$ vanishes at the hard-core radius. The improved wave function is then used to calculate the matrix elements $\langle n'|v|\psi_n\rangle$, and the iteration is continued by recalculating the function $F(r)$. The convergence of the method will be discussed in sect. 7.

Because of the hard core, we have to use a limiting procedure in calculating the matrix elements. Eden and Emery [2]), who considered virtually the same equation, used a perturbation treatment. Such a perturbation treatment is unnecessary as can be seen by considering the hard core as a limiting case of a finite vertical core. A simple manipulation of eq. (19) shows that in the limit of a hard core, one obtains for the matrix elements the expression

$$\langle n'l|t^{NL}|nl\rangle \equiv \langle n'l|v|\psi_{nl}^{NL}\rangle = \frac{\hbar^2}{2\mu}\left[\phi_{n'l}(r)\frac{\mathrm{d}\psi_{nl}^{NL}}{\mathrm{d}r}\right]_{r=c} + \int_0^c \phi_{n'l}(r)\bar{F}(r)\mathrm{d}r + \int_c^\infty \phi_{n'l}(r)v(r)\psi_{nl}^{NL}(r)\mathrm{d}r,$$

$$\bar{F}(r) = -\Delta\phi_{nl}(r) + F(r). \tag{24}$$

The t-matrix between two-particle states $\phi(\boldsymbol{r}, \boldsymbol{R})$ of the type (13) is now calculated by use of (24). Multiplying $\phi(\boldsymbol{r}, \boldsymbol{R})$ by two-particle spin and isospin functions and including the exchange term, one finds

$$\langle n_1' l_1' n_2' l_2'|t^{\Lambda ST}|n_1 l_1 n_2 l_2\rangle = \sum_{n'nlNL}[1-(-1)^{l+S+T}]\langle n_1' l_1' n_2' l_2'; \Lambda|n'lN'L; \Lambda\rangle \times \langle n_1 l_1 n_2 l_2; \Lambda|nlNL; \Lambda\rangle\langle n'l|v^{ST}|\psi_{nl}^{NL\Lambda ST}\rangle. \tag{25}$$

The effect of the exchange term is to require that $l+S+T$ is odd. A similar treatment is used for other types of matrix elements that are needed in sect. 6. For example, defining $\chi(\boldsymbol{r}, \boldsymbol{R}) = \phi(\boldsymbol{r}, \boldsymbol{R}) - \psi(\boldsymbol{r}, \boldsymbol{R})$ and proceeding as above, we find

$$\langle \chi_{n_1' l_1' n_2' l_2'}^{\Lambda ST}|R^2|\chi_{n_1 l_1 n_2 l_2}^{\Lambda ST}\rangle = \sum_{\substack{nlNL \\ n'N'}}[1-(-1)^{l+S+T}]\langle n_1' l_1' n_2' l_2'; \Lambda|n'lNL; \Lambda\rangle \times \langle n_1 l_1 n_2 l_2; \Lambda|nlNL; \Lambda\rangle \int_0^\infty [\chi_{n'l}(r)\chi_{nl}(r)]\mathrm{d}r\langle N'L|R^2|NL\rangle, \tag{26}$$

where $\chi_{nl}(r)$ stands for $\phi_{nl}(r) - \psi_{nl}^{NL\Lambda}(r)$.

5. Calculation of higher-order diagrams

In the preceding sections, we have described how to accurately calculate the reaction matrix, which gives the first-order contribution to the energy in the Brueckner-Goldstone expansion. We now consider higher-order diagrams in this expansion.

We first consider diagrams (d) of fig. 1, which are peculiar to finite nuclei. Their contribution Δ_{ph} to the ground-state energy is

$$\Delta_{\mathrm{ph}} = -\sum_{ak}\frac{|\mathscr{M}_{ak}|^2}{E_a - E_k - C_k}, \tag{27}$$

$$\mathscr{M}_{ak} = \sum_n \langle an|t|kn-nk\rangle - \langle a|U_0|k\rangle. \tag{28}$$

Here and subsequently, we use the convention that states $a, b, c, \ldots$ are unoccupied, and states k, l, m, $n, \ldots$ are occupied. An index such as a stands for $(n_a l_a m_a \sigma_a \tau_a)$, where σ and τ are spin and isospin projections, respectively.

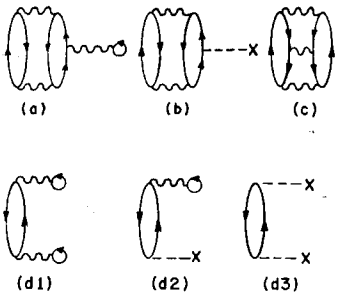

Fig. 1. Correction terms to the first-order Brueckner-Goldstone theory.

The Hartree-Fock self-consistency condition requires that the two terms on the right-hand side of eq. (28) exactly cancel. Thus in a fully self-consistent treatment, diagrams (d) of fig. 1 would add up to zero. By explicitly calculating these terms, we partially correct for the fact that our single-particle potential and wave functions are *not* completely self-consistent.

On summing over all magnetic quantum numbers $m\sigma\tau$, eq. (27) becomes

$$\Delta_{\mathrm{ph}} = -\sum_{\{ak\}} \frac{4(2l_k+1)}{E_a - E_k - C_k} |M_{ak}|^2, \tag{29}$$

$$M_{ak} = \delta(l_a, l_k) \sum_{\{n\}} \sum_{\Lambda ST} \frac{2\Lambda+1}{2l_k+1} \frac{2S+1}{2} \frac{2T+1}{2} \langle n_a l_a n_n l_n | t^{\Lambda ST} | n_k l_k n_n l_n \rangle$$
$$- \langle n_a l_a | \tfrac{1}{2} m\omega^2 r^2 | n_k l_k \rangle, \tag{30}$$

where the matrix element of $t^{\Lambda ST}$ is given by (25). The braces $\{\ \}$ around summation indices indicate that only the quantum numbers nl corresponding to these indices (and not $m\sigma\tau$) are to be summed over. Here the oscillator term contributes only when the particle from below the Fermi surface scatters two shells upwards. This contribution is almost exactly canceled by the two-body part of M_{ak} for reasonable values of $\hbar\omega$. On the other hand, the contributions from higher intermediate states are small because the two-body matrix elements change sign and the Moshinsky brackets become small. The appearance of C_k in the energy denominator also helps in making these contributions small.

Of the third-order diagrams, we only evaluate the ones that are not contained in the three-body cluster summation [7]). These are the hole-hole diagram of fig. (1c) and the U diagram (1b). The contribution from diagram (1c) is

$$\Delta_{\mathrm{hh}} = \tfrac{1}{4} \sum_{\{klmn\}} \sum_{\Lambda ST} (2\Lambda+1)(2S+1)(2T+1) \langle \chi^{\Lambda ST}_{n_i l_i n_m l_m} | \chi^{\Lambda ST}_{n_k l_k n_n l_n} \rangle$$
$$\times \langle n_k l_k n_n l_n | t^{\Lambda ST} | n_l l_l n_m l_m \rangle. \tag{31}$$

Here, both matrix elements contain both direct and exchange terms as explained at the end of sect. 4.

The U diagram gives the contribution

$$\Delta_u = -\sum_{\substack{l,m\\a,b,c}} \langle lm|t\frac{Q}{e}|ab\rangle\langle b|U_0|c\rangle\langle ac|\frac{Q}{e}t|lm-ml\rangle. \tag{32}$$

Since U_0 is a one-body operator, we can write

$$\langle b|U_0|c\rangle = \sum_{a'} \langle ab|U_0(2)|a'c\rangle,$$

where $U_0(2)$ depends only upon the second coordinate r_2. Using this trick, we can write

$$\begin{aligned}\Delta_u &= -\sum_{\substack{l,m\\a,a',b,c}} \langle\chi_{lm}|ab\rangle\langle ab|U_0(2)|a'c\rangle\langle a'c|\chi_{lm}-\chi_{ml}\rangle \\ &= -\sum_{l,m}\langle\chi_{lm}|U_0(2)|\chi_{lm}-\chi_{ml}\rangle. \end{aligned}\tag{33}$$

It is clear that in (33) we may replace $U_0(2)$ by

$$\tfrac{1}{2}[U_0(1)+U_0(2)] = \tfrac{1}{2}m\omega^2(R^2+\tfrac{1}{4}r^2).$$

Making this replacement and summing over magnetic quantum numbers, we obtain

$$\Delta_u = -\sum_{\{lm\}}\sum_{AST}(2\Lambda+1)(2S+1)(2T+1)\langle\chi^{AST}_{n_il_in_ml_m}|\tfrac{1}{2}m\omega^2(R^2+\tfrac{1}{4}r^2)|\chi^{AST}_{n_il_in_ml_m}\rangle, \tag{34}$$

where the last matrix element includes an exchange term and is calculated as in eq. (26). Diagrams with repeated U_0 insertions in particle lines should be smaller than this by a factor of order $\hbar\omega/\bar{e}$, where $\bar{e}$ is a typical two-particle excitation energy and is therefore several hundred MeV. Köhler [11]) has recently given a method for summing repeated U_0 insertions.

6. Calculation of r.m.s. radius

To calculate the r.m.s. radius, we use the expansion for one-body operators that was given by Thouless [12]). The operator in question here is

$$\tilde{O} = \frac{1}{A}\sum_{j=1}^{A} r_j^2 = \frac{1}{A}\sum_{pq}\langle p|r^2|q\rangle a_p^\dagger a_q. \tag{35}$$

Strictly speaking we should use the operator

$$\frac{1}{A}\sum_i (\boldsymbol{R}-\boldsymbol{r}_i)^2 = \frac{1}{A}\sum_i r_i^2 - R^2, \tag{36}$$

where $\boldsymbol{R}$ is the c.m. vector of the nucleus. However, we shall assume that to good approximation the unperturbed Slater-determinant ground state will have the same

c.m. motion as the exact ground state, thus we need to evaluate $\langle R^2 \rangle$ only in the unperturbed ground state.

To evaluate the expectation value of $\tilde{O}$, we have to draw all possible diagrams in which either the interactions or the U lines are replaced by a dot representing the operator $\tilde{O}$. The diagrams that are considered here are given in fig. 2. The total

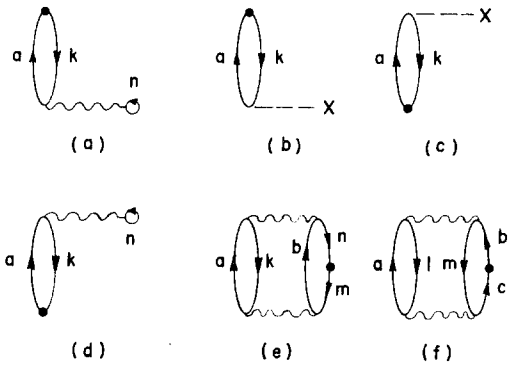

Fig. 2. Diagrams for a one-body operator.

contribution from diagrams (a)–(d) is given by

$$\Delta r^2_{\rm ph} = -\frac{2}{A}\sum_{ak}\frac{\langle k|r^2|a\rangle \mathscr{M}_{ak}}{E_a - E_k - C_k}, \tag{37}$$

where $\mathscr{M}_{ak}$ is defined by (28). The sum over magnetic quantum numbers leads to

$$\Delta r^2_{\rm ph} = -\frac{2}{A}\sum_{\{ak\}}\frac{4(2l_k+1)}{E_a - E_k - C_k}\langle n_k l_k|r^2|n_a l_a\rangle M_{ak}, \tag{38}$$

where M_{ak} is given by (30).

The contribution from diagram 2(e) can be written

$$\Delta r^2_{\rm h} = -\frac{1}{A}\sum_{\{kmn\}}\langle n_m l_m|r^2|n_n l_n\rangle \sum_{\Lambda ST}(2\Lambda+1)(2S+1)(2T+1)$$
$$\times \langle \chi^{\Lambda ST}_{n_k l_k n_n l_n}|\chi^{\Lambda ST}_{n_k l_k n_m l_m}\rangle, \tag{39}$$

where the last matrix element is defined in analogy with (26). The contribution of diagram 2(f) to $\langle r^2 \rangle$ is

$$\Delta r^2_{\rm p} = -2(Am\omega^2)^{-1}\Delta_u, \tag{40}$$

where Δ_u is given by (34).

7. Convergence and accuracy of the method

The iteration procedure described in sect. 4 was started by using a state-independent separation distance to calculate the first approximation for the inhomogeneous term.

Later it was found that the iteration could be equally well started by having $F(r) = 0$ for reasonable values of Δ. The convergence of the procedure depends sensitively upon the parameter Δ. For physical cases ($|\Delta| \approx 100$ MeV), only two iterations were necessary. However for small values of $|\Delta|$, the convergence was extremely slow. One such case is shown in fig. 3. It shows the matrix elements $\langle n0|t|10\rangle$ calculated

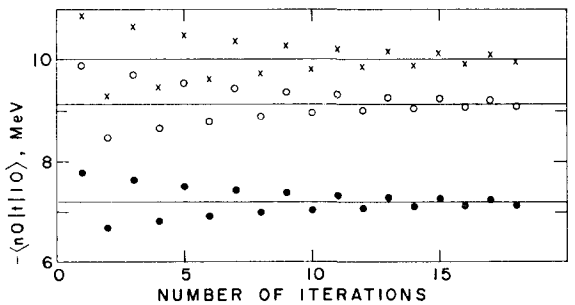

Fig. 3. Study of the convergence of the iteration method for a small value of $|\Delta|$. Here $\Delta = -60$ MeV and $\hbar\omega = 14$ MeV. The three matrix elements plotted are $-\langle n0|t|10\rangle$, $N = L = 0$; the crosses, open circles and solid circles correspond to $n = 0, 1, 2$, respectively.

from (24) for $n = 0, 1, 2$, plotted against the number of iterations. The value of Δ is -60 MeV and $N = L = 0$. The salient feature of the method is that the answer accurate to four figures can be obtained from the first three iterations by taking the average. The average of the first two iterations already gives 0.5 % accuracy, which is certainly enough. The method was found to work equally well for P- and D-waves.

The numerical integration was performed on the CDC-3600 computer, and the differential equations were solved by employing the Argonne library subroutine DIFSUB. No attempt was made to reduce computing time to a minimum for these matrix elements, e.g. by using the coarsest possible mesh consistent with accuracy. But such an attempt *was* made in the nuclear-matter calculations (sect. 9), where it was found that a single matrix element could be calculated in about 1 sec. The minimum time required to calculate a single matrix element in a finite nucleus should be about the same.

In order to get some feeling about how the method works, we applied it to light nuclei. In this calculation we used the S-wave interaction [5]) (with core radius 0.45 fm)

$$\left.\begin{aligned} V_s &= -277.07 \exp\{-2.211(r-0.45)\} \\ V_t &= -549.26 \exp\{-2.735(r-0.45)\} \end{aligned}\right\} \quad \text{for} \quad r > 0.45 \text{ fm}, \tag{41}$$

where the subscripts s and t stand for singlet and triplet, respectively. This interaction has been used with variational calculations on light nuclei [5,13]).

It is instructive to compare various approximation methods. The simplest is the state-dependent separation method [14]), where for simplicity we set $\Delta = 0$. Next is the case in which we neglect the Pauli principle but use a finite value of Δ. Since this

TABLE 2

Comparison of ^{16}O matrix elements $\langle n'l|t|nl\rangle$ for $N = L = l = 0$, $n = 1$ and various values of n'

$\langle n'l\|t\|nl\rangle$	Present method	Eden and Emery	Separation method	RSM
$\langle 00\|10\rangle$	−8.05	−8.24	−7.37	−9.70
$\langle 10\|10\rangle$	−7.52	−7.69	−7.25	−9.06
$\langle 20\|10\rangle$	−6.13	−6.27	−6.41	−7.37
$\langle 30\|10\rangle$	−4.47	−4.57	−5.38	−5.38
$\langle 40\|10\rangle$	−2.77	−2.91	−4.32	−3.33
$\langle \chi\|\chi\rangle$	0.013	0.015		0.035
$\langle \chi\|r^2\|\chi\rangle$	0.014 fm^2	0.043 fm^2		0.054 fm^2

Here $\chi(r)$ is the relative defect wave function for $n = 1$. The oscillator parameter $\hbar\omega = 12$ MeV.

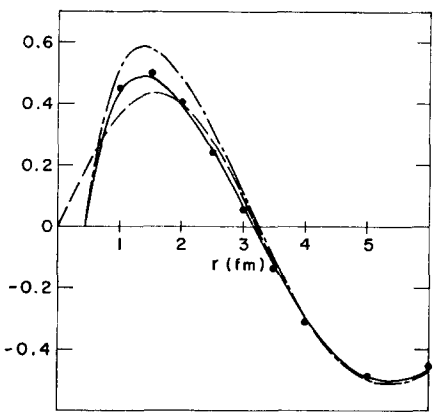

Fig. 4. The wave functions corresponding to table 2 for state $|nlNL\rangle = |1000\rangle$. The dashed line represents the uncorrelated oscillator wave function. The dot-and-dash curve is the RSM approximation to the correlated wave function. The solid curve is the correlated wave function calculated by the method of the present paper. The solid circles are obtained by the present method except that the Eden-Emery approximation is used for the $P_l^{NLA}(n)$.

TABLE 3

Comparison of odd-state matrix elements for $\hbar\omega = 14$ MeV and $\Delta = -125$ MeV in ^{16}O

$\langle n'l\|t\|nl\rangle$	Exact$^+$	Exact$^-$	Separation method$^+$	RSM$^+$	RSM$^-$	cc$^+$	cc$^-$
$\langle 01\|01\rangle$	2.66	−2.99	+2.7	2.48	−3.26	0.13	0.37
$\langle 11\|01\rangle$	3.41	−3.83	+3.4	3.17	−4.19	0.21	0.57
$\langle 21\|01\rangle$	3.68	−4.13	+3.6	3.41	−4.52	0.28	0.75
$\langle 31\|01\rangle$	3.72	−4.14	+3.6	3.44	−4.54	0.33	0.90

The plus and minus signs refer to attractive and repulsive potentials, respectively. The columns labeled cc$^+$ and cc$^-$ give the core contributions for repulsive and attractive potentials [sum of first and second terms of eq. (24)].

method is analogous to the reference-spectrum method [9,15]), we call it RSM. Finally the Eden-Emery approximation is obtained from eq. (19b) by rounding off each number $P_{nl}^{NL\Lambda}(n')$ to either 0 or 1. Table 2 compares the aforementioned approximation methods in the case of the ^{3}S force for the matrix elements $\langle n'0|\,^3t\,|10\rangle$. Corresponding wave functions are plotted in fig. 4. One should in particular note that the RSM predicts far too big a "wound" in the wave function. This would give very large correction terms in sect. 5. The relative P-state case was studied with the same ^{3}S potential. To get the repulsive case we simply reversed the sign of the force. The results for the matrix elements $\langle n'l|t|0l\rangle$ are given in table 3. This odd-state calculation is, of course, entirely unrealistic and was performed only for illustration of the method.

From this study, we conclude that the Eden-Emery approximation is sufficiently accurate for treating the Pauli principle in the case of central forces. The RSM overestimates the matrix element by about 10–15 %. But even so, it provides a convenient starting approximation. Because the RSM gives far too large a defect wave function, one cannot use it to calculate the higher-order correction terms. In this connection, one should notice that even though the Eden-Emery method gives good accuracy for the t-matrix elements, it predicts a quite wrong value for the matrix element $\langle\chi|r^2|\chi\rangle$, which is needed in the evaluation of the U diagram in eq. (34). The reason is that even small errors in the Pauli principle affect the asymptotic behavior of the correlation function.

The fact that the dependence of the matrix elements upon Δ is weak gives a justification for the second assumption stated after eq. (13). However the approximation involved in the first assumption is somewhat more difficult to evaluate. We may make use of the fact that the term

$$F(\boldsymbol{r}, \boldsymbol{R}) \equiv \langle \boldsymbol{r}\boldsymbol{R}|(1-Q)v|\psi\rangle,$$

is a perturbation small enough to be treated iterationally as in the present paper.

Let us first relax approximation 1 and write the Bethe-Goldstone wave function in all its complexity, i.e. in the form

$$\psi^{\Lambda}(\boldsymbol{r}, \boldsymbol{R}) = \psi_0^{\Lambda}(\boldsymbol{r}, \boldsymbol{R}) + \bar{\psi}^{\Lambda}(\boldsymbol{r}, \boldsymbol{R}),$$

$$\psi_0^{\Lambda}(\boldsymbol{r}, \boldsymbol{R}) = \sum_{nlNL} \langle n_1 l_1 n_2 l_2, \Lambda|nlNL, \Lambda\rangle [\psi_{nl}^{NL\Lambda}(\boldsymbol{r})\phi_{NL}(\boldsymbol{R})]^{\Lambda},$$

$$\bar{\psi}^{\Lambda}(\boldsymbol{r}, \boldsymbol{R}) = \sum_{lNL}^{\infty} [\bar{\psi}_l^{NL\Lambda}(\boldsymbol{r})\phi_{NL}(\boldsymbol{R})]^{\Lambda}.$$

Here $\bar{\psi}^{\Lambda}$ contains all the components $\phi_{NL}(\boldsymbol{R})$ of c.m. motion not present in the unperturbed wave function $\phi^{\Lambda}(\boldsymbol{r}, \boldsymbol{R})$. We notice first that in the calculation of the diagonal t-matrix elements only the first part $\psi_0^{\Lambda}(\boldsymbol{r}, \boldsymbol{R})$ is needed. Second, after some algebra similar to that in sect. 3, one finds that approximation 1 can be replaced by a milder one. In calculating the term $F(\boldsymbol{r}, \boldsymbol{R})$, we neglect the second component $\bar{\psi}^{\Lambda}(\boldsymbol{r}, \boldsymbol{R})$ of the Bethe-Goldstone wave function. With this assumption, we shall obtain the same equations for the relative wave functions $\psi_{nl}^{NL\Lambda}$ contained in $\psi_0^{\Lambda}(\boldsymbol{r}, \boldsymbol{R})$ as before. But in addition we also obtain equations for the other components $\bar{\psi}_{nl}^{NL\Lambda}(\boldsymbol{r})$.

These components would be zero except for the fact that the operator $(1-Q)$ is not diagonal in NL. Thus there exist small but non-zero t-matrix elements that are off diagonal in NL, and these will modify $F(\boldsymbol{r}, \boldsymbol{R})$. Wong has calculated one of these matrix elements to be about 5 % as large as matrix elements diagonal in NL (as shown in ref. [9]), table 2). Thus our approximation 1 may produce an error of the order of 5 % in $F(\boldsymbol{r}, \boldsymbol{R})$. This would produce an error in the t-matrix elements of only 5 % of the error in the RSM, i.e. about 0.05 MeV. However, more detailed calculations are required to eliminate all uncertainty on this point, especially since the errors are somewhat larger when the tensor force is taken into account (as can be seen in ref. [9]), table 4).

8. Calculation of binding energy

As a final application, we discuss the calculation of the binding energy of ^{4}He and ^{16}O. The purpose of this calculation is to illustrate the method not to show how well the results agree with experiment (though accidentally they do). But the force is not too unrealistic. In fact, one would get a fairly realistic force by simply adding an odd-state LS force to obtain proper LS splitting of the single-particle states.

For convenience, we write down detailed expressions used in the calculations. The expression for the single-particle potential is given by eqs. (2) and (3). For central forces, eq. (2) becomes

$$\langle k|U|k\rangle = \sum_{\{n\}} \sum_{\Lambda ST} \frac{2\Lambda+1}{2l_k+1} \frac{2S+1}{2} \frac{2T+1}{2} \langle n_k l_k n_n l_n | t^{\Lambda ST} | n_k l_k n_n l_n \rangle$$

$$= C_k + \langle n_k l_k | \tfrac{1}{2} m\omega^2 r^2 | n_k l_k \rangle. \tag{42}$$

This formula shows how to construct the C_k from calculated matrix elements of t.

For S-wave forces, expressions for total kinetic energy T, total potential energy P.E. and single-particle potential energies have been derived for ^{4}He and ^{16}O. We have used the notation

$$M_{l_1 l_2}(nlNL) = \langle nl|t^{NL}|nl\rangle, \tag{43}$$

where (l_1, l_2) specifies the single-particle states involved in the diagonal matrix element; there is no need to specify (n_1, n_2) because these are always zero for occupied states in ^{4}He and ^{16}O. For ^{4}He, the expressions are

$$T = 2.25\hbar\omega,$$

$$\langle 1s|U|1s\rangle = 1.5 M_{ss}(0000),$$

$$\text{P.E.} = 3 M_{ss}(0000).$$

For ^{16}O, the expressions are

$$T = 17.25\hbar\omega,$$

$$\langle 1s|U|1s\rangle = \tfrac{9}{4} M_{sp}(0001) + \tfrac{3}{2} M_{ss}(0000) \approx \tfrac{9}{4} M_{sp}(0000) + \tfrac{3}{2} M_{ss}(0000),$$

$$\langle 1p|U|1p\rangle = \tfrac{1}{4}M_{pp}(0010)+\tfrac{1}{4}M_{pp}(1000)+\tfrac{5}{4}M_{pp}(0002)+\tfrac{3}{4}M_{sp}(0001)$$
$$\approx \tfrac{3}{2}M_{pp}(0010)+\tfrac{1}{4}M_{pp}(1000)+\tfrac{3}{4}M_{sp}(0000),$$
$$\text{P.E.} = 9M_{pp}(0010)+9M_{sp}(0000)+1.5M_{pp}(1000)+3M_{ss}(0000).$$

In the case of ^{16}O, we used the approximations $M(0001) \approx M(0000)$ and $M(0002) \approx M(0010)$ because the numbers $P(n)$ are almost identical. Table 4 shows one iteration step in the case of ^{16}O. In the first column, we indicate which single-particle orbits are involved and in the third column the matrix elements defined by eq. (43). The binding energy per particle is given in fig. 5 with the contributions from

TABLE 4

One iteration step for ^{16}O for $\hbar\omega = 14$ MeV

$(l_1\, l_2)$	$nl\ NL$	$M(nl\ NL)$	C_s	C_p	E_s+C_s	E_p+C_p
S S	00 00	−15.44	−68.9	−56.3	−47.9	−21.3
S P	00 01	−15.63				
P P	00 10	−16.30				
P P	10 00	−10.35				

The input values for parameters C are $C_s = -68.1$ MeV and $C_p = -56.8$ MeV. The matrix elements $M(nl\ NL)$ are defined according to eq. (43).

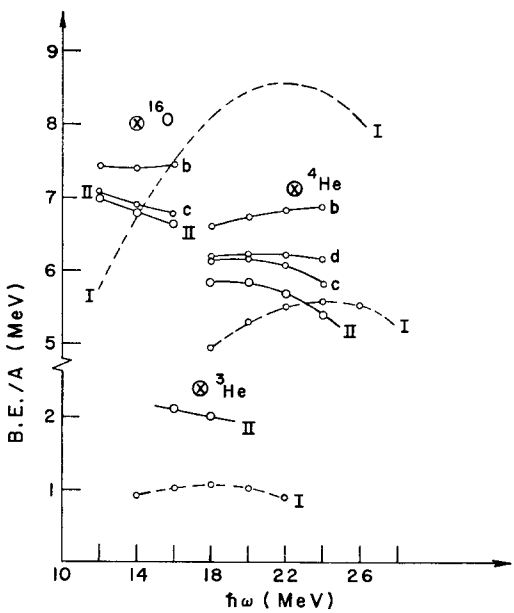

Fig. 5. Binding energy per particle for ^{3}He, ^{4}He and ^{16}O. The circled crosses give the experimental value for ^{16}O and the result of the variational calculation for ^{3}He and ^{4}He. Curve I: First-order separation method, Curve II: Exact t-matrix. c: II+diagram (c) of fig. 1, d: c+diagrams (d), b: c or d+diagram (b).

various correction terms. For ^{16}O, we did not calculate the correction Δ_{ph}. The binding energy of ^{4}He is very sensitive to errors in matrix elements. For instance if we disregard the parameter Δ entirely, ^{4}He will be overbound by 10 MeV. Furthermore the defect wave function $\phi - \psi$ becomes very large and thereby gives rise to very large values for the correction terms. On the other hand, when one treats Δ self-consistently, these correction terms are reasonably small as is seen from fig. 5.

Finally there is the problem of determining the oscillator parameter $\hbar\omega$ and the r.m.s. radius. Ordinarily one calculates the binding energy as a function of $\hbar\omega$ and then reads the equilibrium value from the energy minimum [2,16,17]). The present calculation shows that the result of such a procedure depends on precisely what approximation is used for the total energy. Comparing curves I and II of fig. 5 which give the respective results of the separation method and the self-consistent calculation, one would predict entirely different values of $\hbar\omega$ and hence of the nuclear radius in the two cases. The difference becomes even larger in the case of ^{16}O. Here one can also take the viewpoint [2,6]) that the binding energy and r.m.s. radius should be independent of $\hbar\omega$. In fact, since the Brueckner t-matrix expansion is based on perturba-

TABLE 5

The contributions of various correction terms for the r.m.s. radius of ^{4}He

$\hbar\omega$	18	20	22	24
RMS_0	1.61	1.52	1.45	1.39
Δr_{ph}^2	0.021	0.093	0.161	0.266
Δr_h^2	−0.196	−0.192	−0.197	−0.195
Δr_p^2	+0.106	0.103	0.103	0.100
RMS	1.58	1.53	1.47	1.45

tion theory, there is no extremum principle [18]) for the total energy †. Taking this standpoint, we have added several correction terms to the first-order calculation to see if the results for the binding energy and r.m.s. radius become independent of $\hbar\omega$. We obtained results only for the two nuclei. In each case the binding energy is rather insensitive to $\hbar\omega$; the problem of the r.m.s. radius was studied carefully only in the case of ^{4}He. Unfortunately the uncertainties due to the c.m. motion [13]) of the whole nucleus will interfere for such a light nucleus. The results for the r.m.s. radius are given in table 5. It is seen that the final values of r.m.s. radii vary somewhat less with $\hbar\omega$ than do the values in the first row. This is due to the first correction term Δr_{ph}^2, which tries to correct the erroneous tails of the single-particle wave functions. We might determine the best value of $\hbar\omega$ by requiring that the sum of the correction terms should vanish. This requirement is satisfied for $\hbar\omega \approx 20$–21 MeV and r.m.s. radius ≈ 1.50 fm. The value from variational calculations [5]) is 1.48 fm.

† Brandow [18]) argues that minimizing the energy with respect to $\hbar\omega$ is correct only when the appropriate approximation is used for the energy.

Finally, the ground-state energy should be corrected for the effects of zero-point vibrations. In ^{16}O, these are estimated [19]) to contribute about -1 MeV/A.

9. Application to nuclear matter

The method described in sects. 3 and 4 can also be used to calculate the t matrix in infinite nuclear matter. The basic equations are formally identical to eqs. (4)–(6). However, the unperturbed wave function ϕ is now given by

$$\phi = \exp(i\boldsymbol{k}_0 \cdot \boldsymbol{r})\chi^S_{m_s} = \langle \boldsymbol{r}|\boldsymbol{k}_0 S m_s\rangle. \tag{44}$$

Here we have explicitly indicated that the two nucleons are coupled to total spin S with projection m_s because we want to allow for the possibility of a tensor force.

We assume that the single-particle energy of unoccupied states with $k > k_F$ is pure kinetic energy. Hence the operator e becomes [8])

$$e = \gamma^2 - \nabla^2, \tag{45}$$

where γ^2 is a positive constant. Applying e to both sides of eq. (6) and using eqs. (44) and (45) gives

$$(\nabla^2 - \gamma^2 - v)\psi = -(\gamma^2 + k_0^2)\phi - (1-Q)v\psi. \tag{46}$$

The iteration procedure is now the same as described previously. In the first iteration, $(1-Q)v\psi$ is neglected (RSM); and in the nth iteration, $(1-Q)v\psi$ is calculated from the result of the $(n-1)$st iteration.

We must now decompose each term of (46) into partial waves. For $\phi = \langle \boldsymbol{r}|\boldsymbol{k}_0 S m_s\rangle$ and ψ, we have

$$\left.\begin{matrix}\langle \boldsymbol{r}|\boldsymbol{k}_0 S m_s\rangle \\ \psi_{Sm_s}(\boldsymbol{k}_0, \boldsymbol{r})\end{matrix}\right\} = \sum_{JL} i^L[4\pi(2L+1)]^{\frac{1}{2}}(LS0m_s|Jm_s) \left\{\begin{matrix} j_L(k_0 r)\mathscr{Y}^{m_s}_{JLS}(\hat{\boldsymbol{k}}_0, \hat{\boldsymbol{r}}) \\ \\ \sum_{L'} r^{-1} u^{JS}_{LL'}(k_0, r)\mathscr{Y}^{m_s}_{JL'S}(\hat{\boldsymbol{k}}_0, \hat{\boldsymbol{r}}). \end{matrix}\right\} \tag{47}$$

Here we have coupled $Y_{L0}(\hat{\boldsymbol{k}}_0, \hat{\boldsymbol{r}})$, which occurs in the partial wave expansion of $\exp(i\boldsymbol{k}_0 \cdot \boldsymbol{r})$, to $\chi^S_{m_s}$ to obtain an eigenfunction of J, L, S, and $J_Z = m_s$. According to (47), if ϕ has "entrance channel" quantum numbers $LJSJ_Z$, then ψ will have the same JSJ_Z, but the tensor force will mix in different L-values [20]) †. Thus the correlated wave $u^{JS}_{LL'}$ in channel L' corresponds to the unperturbed wave in channel L.

In order to treat the term $(1-Q)v\psi$ in (46), we shall need a partial wave expansion for

$$\langle \boldsymbol{k}Sm_s'|t|\boldsymbol{k}_0 S m_s\rangle = \langle \exp(i\boldsymbol{k}\cdot\boldsymbol{r})\chi^S_{m_s'}|v|\psi_{Sm_s}(\boldsymbol{k}_0, \boldsymbol{r})\rangle. \tag{48}$$

Total spin is conserved, but its projection is not. Here m_s' and m_s are both defined relative to polar axis $\hat{\boldsymbol{k}}_0$. In the expansion of $\exp(i\boldsymbol{k}\cdot\boldsymbol{r})$, there occurs $Y_{L0}(\hat{\boldsymbol{k}}, \hat{\boldsymbol{r}})$.

† See ref. [8]), sect. 6.

This must be expressed in terms of $Y_{LM}(\hat{\boldsymbol{k}}_0, \hat{\boldsymbol{r}})$ (by using the addition theorem for spherical harmonics) before it is coupled to $\chi^S_{m_s'}$. When this is done and use is made of

$$v|u^{JS}_{LL'}(r)\mathscr{Y}^{m_s}_{JL'S}\rangle = \sum_{L''}\langle JL'S|v(r)|JL'S\rangle|u^{JS}_{LL'}(r)\mathscr{Y}^{m_s}_{JL''S}\rangle, \tag{49}$$

eq. (48) becomes

$$\langle \boldsymbol{k}Sm_s'|t|\boldsymbol{k}_0Sm_s\rangle = \sum_{JLL'} i^{L-L'}[4\pi(2L+1)]^{\frac{1}{2}}(L'Sm_s - m_s'm_s'|Jm_s) \times (LS0m_s|Jm_s)Y_{L'm_s-m_s'}(\hat{\boldsymbol{k}}, \hat{\boldsymbol{k}}_0)t^{JS}_{LL'}(k, k_0), \tag{50}$$

where

$$t^{JS}_{LL'}(k, k_0) = 4\pi\sum_{L''}\int_0^\infty rj_{L'}(kr)\langle JL'S|v(r)|JL''S\rangle u^{JS}_{LL''}(k_0, r)\mathrm{d}r. \tag{51}$$

The operator $1-Q \equiv P$ is diagonal in momentum space, and in the angle-average approximation [20]) its eigenvalues are given by

$$P(k, K) = \begin{cases} 1 & \text{for } k \leqq (k_F^2 - \frac{1}{4}K^2)^{\frac{1}{2}} \\ 0 & \text{for } k > k_F + \frac{1}{2}K \\ 1-(k^2+\frac{1}{4}K^2-k_F^2)/(kK) & \text{otherwise,} \end{cases} \tag{52}$$

where k and K are the relative and total momenta, respectively. Thus we have

$$(1-Q)v\psi_{Sm_s}(\boldsymbol{k}_0, \boldsymbol{r}) = \sum_{m_s'}\int\frac{\mathrm{d}^3k}{(2\pi)^3}\mathrm{e}^{i\boldsymbol{k}\cdot\boldsymbol{r}}|\chi^S_{m_s'}\rangle P(k, K) \times \langle\chi^S_{m_s'}\mathrm{e}^{i\boldsymbol{k}\cdot\boldsymbol{r}}|v|\psi_{Sm_s}(\boldsymbol{k}_0, \boldsymbol{r})\rangle. \tag{53}$$

Here we have simply expanded $v\psi$ in the complete set of states $|\boldsymbol{k}Sm_s'\rangle$ and multiplied each of these states by $P(k, K)$. Putting (48) and (50) into (53) now gives

$$(1-Q)v\psi_{Sm_s}(\boldsymbol{k}_0, \boldsymbol{r}) = \sum_{JLL'} i^L[4\pi(2L+1)]^{\frac{1}{2}}(LS0m_s|Jm_s)r^{-1}F_{LL'}(r)\mathscr{Y}^{m_s}_{JL'S}(\hat{\boldsymbol{k}}_0, \hat{\boldsymbol{r}}), \tag{54}$$

where

$$F^{JS}_{LL'}(r) = \frac{1}{2\pi^2}\int rj_{L'}(kr)P(k, K)t^{JS}_{LL'}(k, k_0)k^2\mathrm{d}k. \tag{55}$$

The partial wave form of (46) is now obtained as follows. Substitute (47), (49) and (54) into (46). Then take the scalar product with $\langle\mathscr{Y}^{m_s}_{JL'S}(\hat{\boldsymbol{k}}_0, \hat{\boldsymbol{r}})|$, multiply by $(LS0m_s|Jm_s)$ and sum over m_s. The result is

$$\left[\frac{\mathrm{d}^2}{\mathrm{d}r^2} - \frac{L'(L'+1)}{r^2} - \gamma^2\right]u^{JS}_{LL'}(r) - \sum_{L''}\langle JL'S|v(r)|JL''S\rangle u^{JS}_{LL''}(r) = -\delta_{LL'}(\gamma^2+k_0^2)rj_L(k_0r) - F^{JS}_{LL'}(r). \tag{56}$$

The boundary conditions are

$$u^{JS}_{LL'}(r) = 0 \qquad \text{for} \quad r \leqq c, \tag{57}$$

$$u^{JS}_{LL'}(r) \to \delta_{LL'} r j_L(k_0 r) \qquad \text{as} \quad r \to \infty. \tag{58}$$

In a typical iteration, (56) is solved for $u^{JS}_{LL'}$, and the result is used to calculate $t^{JS}_{LL'}(k, k_0)$ as a function of k from (51). The $t^{JS}_{LL'}(k, k_0)$ are put into (55) to get an improved estimate for $F^{JS}_{LL'}(r)$ to be used in the next iteration. This process is continued until the $t^{JS}_{LL'}(k, k_0)$ no longer change appreciably from one iteration to the next.

Eq. (51) cannot be used as it stands when the potential has a hard core. But eq. (51) can be cast into a practical form † by manipulating eq. (56) and the equation

$$\left[\frac{\mathrm{d}^2}{\mathrm{d}r^2} - \frac{L'(L'+1)}{r^2} + k^2\right] r j_{L'}(kr) = 0. \tag{59}$$

Multiply eq. (56) by $r j_{L'}(kr)$ and eq. (59) by $u^{JS}_{LL'}(r)$, subtract and integrate from $r = 0$ to $r = c+0$, using the fact that $u^{JS}_{LL'}(r) = 0$ for $r \leqq c$. Putting the result into eq. (51) gives

$$t^{JS}_{LL'}(k, k_0) = 4\pi \int_0^c r j_{L'}(kr)[\delta_{LL'}(\gamma^2 + k_0^2) r j_L(k_0 r) + F^{JS}_{LL'}(r)]\mathrm{d}r$$
$$+ 4\pi c j_{L'}(kc) \left[\frac{\mathrm{d}u^{JS}_{LL'}}{\mathrm{d}r}\right]_{r=c} + 4\pi \sum_{L''} \int_c^\infty r j_{L'}(kr) \langle JL'S|v(r)|JL''S\rangle u^{JS}_{LL''}(r)\mathrm{d}r, \tag{60}$$

which can be used for a potential with a hard core.

Eq. (56) is solved in virtually the same way as outlined previously for eq. (19). It is necessary to have asymptotic solutions that are valid when r is so large that $v(r)$ can be neglected. The asymptotic solution of the homogeneous equation is proportional to $h_{L'}(i\gamma r)$. The asymptotic solution of the full inhomogeneous equation is

$$u^{JS}_{LL'}(r) \sim \delta_{LL'} r j_L(k_0 r) + \frac{1}{2\pi^2} \int r j_{L'}(kr) P(k, K) t^{JS}_{LL'}(k, k_0) \frac{k^2 \mathrm{d}k}{\gamma^2 + k^2}. \tag{61}$$

The smooth approach of the iteration procedure to the exact solution illustrated in fig. 3 can be used to increase the rate of convergence. If one assumes that the error in the calculated $t^{JS}_{LL'}(k, k_0)$ is reduced by a constant factor in each iteration, then one can use the results from the three previous iterations to estimate the exact value. Using this estimate in the next iteration increases the rate of convergence.

For the $^1S_0$ and $^3S_1$ entrance-channel states, an error of less than 0.4 MeV · fm^3 in $t^{JS}_{LL}(k_0, k_0)$ was usually achieved in four or five iterations. (This corresponds to an error of 0.01 MeV per particle in the binding energy.) For higher partial waves, fewer iterations were required to attain the same accuracy.

† Cf. ref. [8]), sects. 5 and 6.

Eq. (56) was integrated with a fourth-order Runge-Kutta formula, the mesh used being $r = c(0.05)c+0.8(0.16)c+4.0$, where c is the core radius. For $r > c+4.0$, $u_{LL'}^{JS}(r)$ was approximated by $\delta_{LL'} r j_L(k_0 r)$. The integral (55) was calculated by Simpson's rule, the step size being $\Delta k = 0.3\,\mathrm{fm}^{-1}$. For the Reid new-core potential [21])†, these meshes were adequate to achieve the accuracy mentioned above. To calculate a single matrix element $t_{LL}^{JS}(k_0, k_0)$ on the CDC-3600 computer required about 0.5 sec for uncoupled states and 1.1 sec for coupled states.

We have calculated the binding energy of nuclear matter at normal density ($k_F = 1.36\ \mathrm{fm}^{-1}$) for both the Reid soft-core and new-core potentials [21]). The single-particle energy spectrum used in both cases was

$$E(k) = \begin{cases} \dfrac{\hbar^2 k^2}{2m} & \text{for} \quad k > k_F, \\ \dfrac{\hbar^2 k^2}{2m^*} + A_1 & \text{for} \quad k < k_F, \end{cases} \tag{62}$$

$$m^* = 0.6\, m, \qquad A_1 = -81\ \mathrm{MeV}. \tag{63}$$

This spectrum is very nearly self-consistent. The value of m^* is the same as that obtained by Sprung [22]) in self-consistent calculations with the Reid soft-core potential. Also, this spectrum has $\overline{T}+\frac{1}{2}\overline{U} = -9.8$ MeV, which is not very different from the calculated binding energies of -9.3 MeV and -5.6 MeV for the soft-core and new-core potentials, respectively.

The binding energy involves an integration over the Fermi sea, for which we used the mesh $k_0/k_F = 0(0.125)1.0$. For each value of k_0, K was put equal to its r.m.s. value.

Table 6 shows the contributions of the individual partial waves to the energy per particle and to the average value of the parameter κ defined by

$$\kappa = \rho \int |\phi(\boldsymbol{r}) - \psi(\boldsymbol{r})|^2 \mathrm{d}^3 r, \tag{64}$$

where ρ is the particle density. The value of κ is of interest because it is the expansion parameter of the presently accepted nuclear many-body theory [7,28]).

By using the calculated value of κ, we can correct††) our calculated binding energies for the small deviation of the single-particle energy spectrum from self-consistency. The self-consistent values of the energy per particle are found to be -6.8 MeV and -9.4 MeV for the Reid new-core and soft-core potentials, respectively. To these energies must be added the contributions from three-body correlations, which are believed to be about -1 MeV per particle [7]). Also, the contribution to higher partial

† D. W. Sprung kindly supplied the latest parameters of Reid's new-core potential in the $^3S_1$–$^3D_1$ state.

†† See ref. [8]), sect. 6.

waves is not adequately represented by OPEP, and this may lead to additional binding energy of the order of 1 MeV per particle [24]).

We have compared our results with those recently obtained by Sprung [22,25])†, who uses the RSM with first- and second-order corrections [8,26]). The agreement is excellent, the discrepancy being no larger than 0.1 MeV per particle in any partial wave. Sprung finds the RSM with first-order correction to be accurate to 0.1 MeV in all partial waves except $^3S_1$, for which the error is about 0.5 MeV. For this partial wave, the second-order correction to the RSM is necessary in order to reduce the error below 0.1 MeV.

TABLE 6

Partial-wave contributions to the energy per particle E/A and the parameter κ defined in the text for the Reid new-core and soft-core potentials at $k_F = 1.36$ fm^{-1}

Entrance channel	E/A (MeV)		κ	
	new core	soft core	new core	soft core
$^1S_0$	−14.66	−15.52	0.0380	0.0221
$^1P_1$	3.41	2.38	0.0069	0.0040
$^1D_2$	−2.75	−2.56	0.0002	0.0002
$^3S_1$	−13.12	−14.99	0.1354	0.0978
$^3D_1$	1.47	1.46	0.0001	0.0000
$^3P_0$	−3.96	−3.31	0.0017	0.0023
$^3P_1$	10.64	9.92	0.0054	0.0041
$^3P_2$	−6.82	−7.06	0.0051	0.0040
$^3F_2$	−0.54	−0.56	0.0000	0.0000
$^3D_2$	−4.54	−4.33	0.0004	0.0004
OPEP	2.26	2.26		
SUM	−28.61	−32.31	0.193	0.135
$\bar{T}$	23.01	23.01		
TOTAL E/A	−5.6	−9.3		

The total E/A is obtained by adding the average kinetic energy $\bar{T}$ to the calculated interaction energy. The energy labeled OPEP is calculated in Born approximation by use of the one-pion-exchange potential for all higher partial waves; the result for OPEP quoted here is from ref. [25]).

The present method is of course applicable to a potential with either a hard or soft core. It is more accurate but also more time-consuming than the RSM. And in contrast to the RSM, it gives very accurate two-body wave functions that are needed in three-body calculations [7]). It should be roughly comparable in speed to the Brueckner-Gammel method [20]) or the modified Brueckner-Gammel method which has recently been studied by Dahll, Østgaard and Brandow [27]). Our method has the advantage of treating the hard core exactly; in the Brueckner-Gammel method, an approximation must be made [20]). This approximation appears to be very accurate for small values of γ^2 (for which it reproduces the exact values to better than 0.1 MeV per particle) but becomes worse and worse as γ^2 increases.

† Sprung's recent results for the $^3S_1$ state are slightly different from those quoted in ref. [25]) and agree with those of this paper.

One of the authors (BDD) is grateful to D. W. Sprung for sending him information on the Reid new-core potential as well as detailed results of RSM calculations to aid in checking our computer program for nuclear matter. We are also indebted to R. V. Reid for communicating his nucleon-nucleon potentials.

References

1) A. Kallio and B. D. Day, Phys. Lett. **25B** (1967) 72
2) R. J. Eden and V. J. Emery, Proc. Roy. Soc. **A248** (1958) 266;
R. J. Eden, V. J. Emery and S. Sampanthar, Proc. Roy. Soc. **A253** (1959) 177, 186
3) D. Grillot and H. McManus, preprint
4) A. D. MacKellar and R. L. Becker, Phys. Lett. **18** (1965) 308;
R. L. Becker and A. D. MacKellar, Phys. Lett. **21** (1966) 201;
B. M. Morris and R. L. Becker, Bull. Am. Phys. Soc. **12** (1967) 559
5) Y. C. Tang and R. C. Herndon, Phys. Lett. **18** (1965) 42
6) K. T. R. Davies, S. J. Krieger and M. Baranger, Nucl. Phys. **84** (1966) 545
7) R. Rajaraman and H. A. Bethe, Revs. Mod. Phys. **39** (1967) 745
8) H. A. Bethe, B. H. Brandow and A. G. Petschek, Phys. Rev. **129** (1963) 225
9) C. W. Wong, Nucl. Phys. **A91** (1967) 399, especially eq. (47)
10) A. Erdelyi, Higher transcendental functions Vol. II (McGraw-Hill Book Co., New York, 1953) p. 116
11) H. S. Köhler, Nucl. Phys. **A98** (1967) 569;
H. S. Köhler and R. J. McCarthy, Nucl. Phys. **A106** (1968) 313
12) D. J. Thouless, The quantum mechanics of many-body systems (Academic Press, New York, 1961) p. 47
13) H. J. Mang and W. Wild, Z. Phys. **154** (1959) 182
14) A. Kallio, Phys. Lett. **18** (1965) 51
15) T. T. S. Kuo and G. E. Brown, Nucl. Phys. **85** (1966) 40
16) R. J. McCarthy and H. S. Köhler, Nucl. Phys. **A99** (1967) 65
17) C. W. Wong, Nucl. Phys. **A104** (1967) 417
18) B. H. Brandow, private communication and Revs. Mod. Phys. **39** (1967) 771, sect. X
19) G. E. Brown and C. W. Wong, Nucl. Phys. **A100** (1967) 241;
A. Kallio, Ann. Acad. Sci. Fenn., Ser. A. VI, Physica **163** (1964)
20) K. A. Brueckner and J. L. Gammel, Phys. Rev. **109** (1958) 1023
21) R. V. Reid, private communication
22) D. W. Sprung, private communication
23) B. D. Day, Revs. Mod. Phys. **39** (1967) 719
24) P. Siemens, private communication
25) D. W. Sprung, paper delivered at Int. Conf. on Atomic Masses, Winnipeg (August 1967)
26) D. W. Sprung and P. C. Bhargava, Ann. of Phys. **42** (1967) 222
27) G. Dahll, E. Østgaard and B. H. Brandow, Nucl. Phys., to be published